AGU PUBLICATIONS

JGR

Journal of Geophysical Research: Space Physics

RESEARCH ARTICLE

10.1002/2014JA020048

Special Section:
Long-term Changes and Trends in the Stratosphere, Mesosphere, Thermosphere, and Ionosphere

Key Points:
- Ensemble Empirical Mode Decomposition (EEMD) was applied to f_oF_2 and h_mF_2 data
- EEMD-based and linear regression-based trend analyses were compared
- Long-term decrease in solar activity affects f_oF_2 trends more than h_mF_2 trends

Correspondence to:
I. Cnossen,
inos@bas.ac.uk

Citation:
Cnossen, I., and C. Franzke (2014), The role of the Sun in long-term change in the F_2 peak ionosphere: New insights from EEMD and numerical modeling, *J. Geophys. Res. Space Physics*, *119*, 8610–8623, doi:10.1002/2014JA020048.

Received 4 APR 2014
Accepted 13 SEP 2014
Accepted article online 15 SEP 2014
Published online 16 OCT 2014

The role of the Sun in long-term change in the F_2 peak ionosphere: New insights from EEMD and numerical modeling

Ingrid Cnossen[1] and Christian Franzke[2]

[1]British Antarctic Survey, Cambridge, UK, [2]Meteorological Institute, Center for Earth System Science and Sustainability, University of Hamburg, Hamburg, Germany

Abstract We applied Ensemble Empirical Mode Decomposition (EEMD) for the first time to ionosonde data to study trends in the critical frequency of the F_2 peak, f_oF_2, and its height, h_mF_2, from 1959 to 2005. EEMD decomposes a time series into several quasi-cyclical components, called Intrinsic Mode Functions, and a residual, which can be interpreted as a long-term trend. In contrast to the more commonly used linear regression-based trend analysis, EEMD makes no assumptions on the functional form of the trend and no separate correction for the influence of solar activity variations is needed. We also adopted a more rigorous significance testing procedure with less restrictive underlying assumptions than the *F* test, which is normally used as part of a linear regression-based trend analysis. EEMD analysis shows that trends in h_mF_2 and f_oF_2 between 1959 and 2005 are mostly highly linear, but the *F* test tends to overestimate the significance of trends in h_mF_2 and f_oF_2 in 30% and 25% of cases, respectively. EEMD-based trends are consistently more negative than linear regression-based trends, by 30–35% for h_mF_2 and about 50% for f_oF_2. This may be due to the different treatment of the influence of a long-term decrease in solar activity from 1959 to 2005. We estimate the effect of this decrease in solar activity with two different data-based methods as well as using numerical model simulations. While these estimates vary, all three methods demonstrate a larger relative influence of the Sun on trends in f_oF_2 than on trends in h_mF_2.

1. Introduction

The charged portion of the Earth's atmosphere, the ionosphere, is mainly produced by the absorption of extreme ultraviolet radiation from the Sun. The F_2 layer is the densest part of the Earth's ionosphere. Long-term (multidecadal) changes in the F_2 layer ionosphere have been studied extensively during the past few decades, since the pioneering studies of *Roble and Dickinson* [1989], *Rishbeth* [1990], and *Rishbeth and Roble* [1992]. They predicted that an increase in CO_2 concentration causes cooling of the thermosphere, with the subsequent atmospheric contraction leading to a lowering of ionospheric layers. Initially, observational studies from single stations confirmed that the F_2 peak height, h_mF_2, is indeed lowering [e.g., *Bremer*, 1992; *Ulich and Turunen*, 1997]. However, analysis of many more stations revealed that long-term changes in h_mF_2 vary considerably with location, with some stations even showing positive trends [e.g., *Upadhyay and Mahajan*, 1998]. In addition, significant long-term trends have been observed in the critical frequency of the F_2 layer, f_oF_2 (related to the peak electron density, N_mF_2, as $f_oF_2 \propto \sqrt{N_mF_2}$), even though global cooling and contraction is not expected to have a significant effect on f_oF_2 or N_mF_2 [*Rishbeth*, 1990; *Rishbeth and Roble*, 1992]. These findings indicate that other processes must also contribute to long-term change in the F_2 peak ionosphere. Indeed, changes in the Earth's main magnetic field have now been identified as an important contributor [*Elias and Ortiz de Adler*, 2006; *Cnossen and Richmond*, 2008, 2013; *Cnossen*, 2014]. However, there are also other potential contributors that could be important, such as long-term changes in solar or geomagnetic activity or effects of climatic changes in the atmosphere below. *Laštovička* [2005] noted that for the F_2 layer ionosphere in particular, influences of the Sun may be important, but they have not been quantified before. Therefore, we systematically explore the role of long-term (>11 year) variations in solar activity in causing trends in h_mF_2 and f_oF_2 in some more detail here.

We will do this mainly using a data analysis technique that has not been applied to ionosonde data before. To appreciate the benefits of this new technique, it is useful to first briefly review the most common approach for analyzing long-term trends in ionosonde data, illustrated in Figure 1. The first step of that approach is to

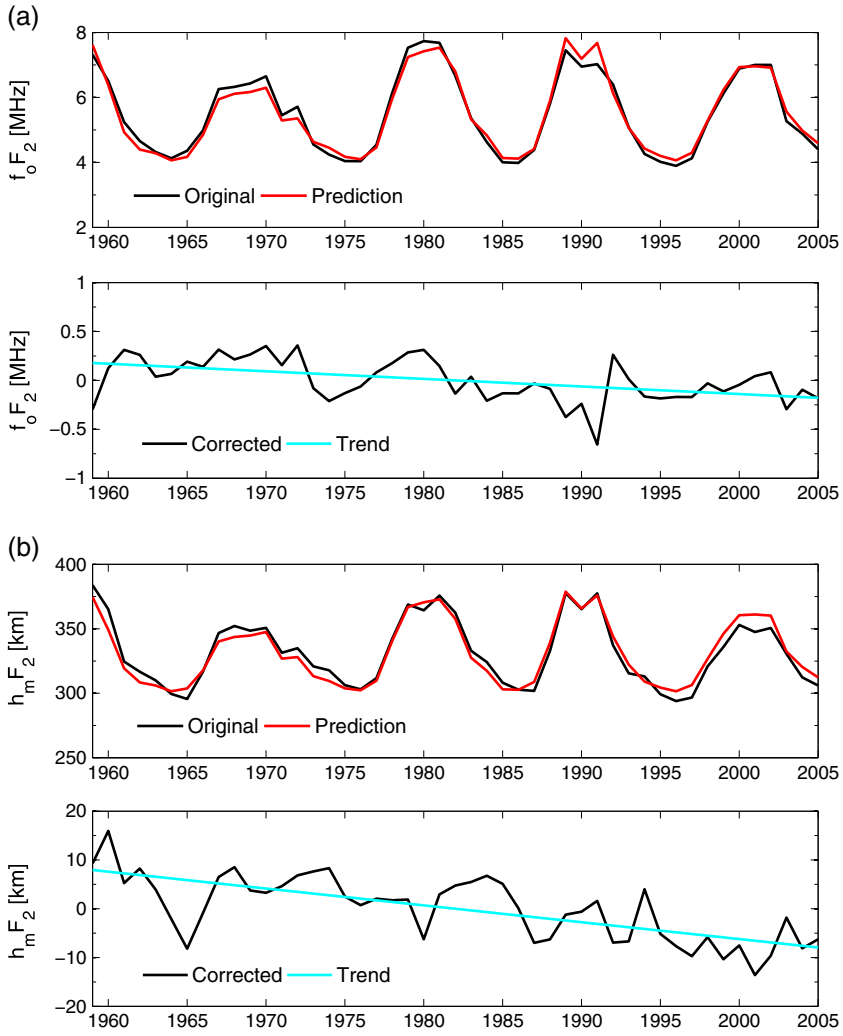

Figure 1. (a) Example of the standard linear regression method applied to annual mean f_oF_2 data from Juliusruh/Rugen averaged over all local times. The original f_oF_2 time series (black) and the prediction based on a linear regression with $F_{10.7}$ (red) (top). The corrected f_oF_2 time series (= original − prediction; black) and the trend obtained from a second linear regression with time (cyan) (bottom). (b) Same as Figure 1a but for h_mF_2 data from Juliusruh/Rugen.

correct the time series to be analyzed for the influence of solar activity variations, which dominate ionosonde data. This is normally done using a linear regression with a solar activity index; i.e., the observed time series is fitted to a function of the form: prediction = a*(solar activity index) + b, with a and b coefficients to be determined from ordinary least squares. Here we will assume the solar activity index to be $F_{10.7}$. A second linear regression on the corrected time series (= original time series − prediction from linear regression with $F_{10.7}$) with time is done to obtain the long-term trend. The statistical significance of the trend is normally determined with an F test.

There are a few potential weaknesses in this approach. First, when the original time series is corrected for the influence of solar activity variations, not only the solar cycle signal is suppressed but also the influence of any longer term changes in solar activity. This may be the reason that long-term variation of solar activity has not been considered much as a contributing cause of long-term trends in h_mF_2 or f_oF_2: it is assumed that any effect of such variation is already removed in this step. However, it is implicitly assumed that a single regression coefficient is appropriate for all timescales of solar activity variations. In other words, the assumption is made that a given change in $F_{10.7}$ will have the same effect on f_oF_2 or h_mF_2, regardless of whether it takes place over a few years or over several decades. This may not necessarily be a valid assumption, and there is therefore a risk that a false signal is introduced in the corrected time series. This would affect the long-term trend that is obtained, as well as obscure any influences of long-term solar

variability on the ionosphere. Two other potential problems with the linear regression approach are that the trend is assumed to be linear, which may not be the case, and that the underlying assumptions of the *F* test are not strictly met by the data, which could potentially make the significance determination unreliable.

The new trend analysis approach we use here circumvents these problems and also offers an opportunity to test how much (or little) of a problem they really are. Central to this new approach is a time series analysis technique called Ensemble Empirical Mode Decomposition (EEMD) [*Huang et al.,* 1998; *Wu and Huang*, 2009]. EEMD can be applied to nonlinear and nonstationary time series and is a data-driven method which decomposes a time series into several quasi-cyclical components, called Intrinsic Mode Functions (IMFs), and a residual. The residual can be interpreted as a long-term trend. EEMD analysis has previously been applied successfully to tropospheric temperature records to analyze long-term trends [*Franzke*, 2010, 2012]. The key advantages of EEMD analysis are that there is no separate correction for the solar cycle needed and no a priori assumptions are made on the functional form of the long-term trend. This may therefore be a better way of extracting the long-term trend signal from a time series dominated by the solar cycle. We also perform a more rigorous significance testing procedure with less restrictive underlying assumptions compared to the *F* test.

The aims of this study are twofold. First, we test some of the assumptions of the standard linear regression approach, which is helpful to assess the quality of trends obtained previously with this method. We then compare trends obtained with the linear regression-based analysis to trends obtained with EEMD analysis. Due to the different treatment of solar influences by these two methods, this naturally provides a first clue on the contribution of the Sun in long-term trends in h_mF_2 and f_oF_2. The second aim of our study is to quantify that contribution more precisely. We do this in two different ways based on data analysis and also offer a third, independent estimate based on numerical model simulations.

The rest of this paper is organized as follows. Section 2 describes the data selection criteria used and initial processing done on the data. Section 3 provides more information about the EEMD technique (3.1), the statistical significance testing procedure (3.2), the data-based methods of estimating the solar contribution to trends (3.3), and the numerical model simulations (3.4). Results are presented in section 4, starting with testing the linearity of trends and the reliability of the *F* test (4.1). Section 4.2 compares the linear regression- and EEMD-based trends, and section 4.3 presents the three different estimates of solar influences on the trends. In section 4.4 we briefly compare trends between stations. We finish with a discussion in section 5 and summarize our main conclusions in section 6.

2. Data

We used ionosonde data for a selected set of stations extracted from the recently published database by *Damboldt and Suessmann* [2012], which gives monthly median values of f_oF_2 and the maximum usable frequency parameter M(3000)F_2. M(3000)F_2 is the ratio of the maximum usable frequency that can be used to transmit a signal over a distance of 3000 km via reflection by the ionosphere to the critical frequency f_oF_2. The *Shimazaki* [1955] formula was used to calculate h_mF_2 from M(3000)F_2:

$$h_mF_2 = \frac{1490}{M(3000)F2} - 176 \tag{1}$$

Empirical formulas like these are routinely used by long-term trend analyses of h_mF_2, as it is a very time consuming task to scale h_mF_2 directly from ionograms [e.g., *Ulich and Turunen*, 1997]. The *Shimazaki* [1955] is the simplest of these formulas; others have been developed that add a correction term for the underlying ionization. However, these rely on knowledge of the critical frequency of the *E* layer, which is not available in the *Damboldt and Suessmann* [2012] database. We are therefore limited to using the *Shimazaki* [1955] formula here. We must bear in mind, however, that it is possible that the use of the *Shimazaki* [1955] formula can introduce some error in the h_mF_2 time series and therefore also possibly in the trends obtained.

The monthly median f_oF_2 and h_mF_2 values were averaged over all months and local times (ignoring any missing data points), in the same way as *Bremer et al.* [2012] did. This serves as a starting point for the new trend analysis technique we are introducing here. Previous studies [e.g., *Ulich and Turunen*, 1997; *Elias and Ortiz de Adler*, 2006] have shown that ionospheric trends do vary with season and local time. In future work, we may consider such dependencies, but this is outside the scope of the present study.

Table 1. Locations of the Stations Included in Our Analysis

Station Name	Latitude (deg)	Longitude (deg)
Syowa Base	−69.0	39.6
Mawson	−67.6	62.9
Port Stanley	−51.7	−57.8
Christchurch	−43.6	172.8
Hobart	−42.9	147.2
Canberra	−35.3	149.0
Mundaring	−32.0	116.2
Townsville	−19.3	146.7
Okinawa	26.3	127.8
Yamagawa	31.2	130.6
Hiratsuka	35.4	139.5
Kokubunji	35.7	139.5
Ashkabad	37.9	58.3
Boulder	40.0	−105.3
Rome	41.8	12.5
Wakkanai	45.4	141.7
Juliusruh/Rugen	54.6	13.4
Moscow	55.5	37.3
Tomsk	56.5	84.9
Leningrad	60.0	30.7
Sodankylä	67.4	26.6

Our selection of stations was based on the following considerations. First, the time interval should be kept the same for all stations to eliminate differences between trends at different stations arising from different periods being analyzed. Second, this time interval should be sufficiently long for the solar cycle to be well established so that it can be recognized by the EEMD technique as such, but not so long that only very few stations would qualify. Also, we wanted to avoid the recent solar minimum period of 2008/2009, which showed unusually low solar activity. Including this period could skew the results, which we considered undesirable. Several other long-term trend studies avoided this period for the same reason [e.g., *Emmert and Picone*, 2011; *Bremer et al.*, 2012]. Third, we allowed only up to 3 years of a time series to be missing. No missing data were allowed at the beginning or end of a time series. Based on these criteria, we selected the interval from 1959 to 2005 (47 years). There were 21 stations with sufficient data for f_oF_2 and 19 stations with sufficient data for h_mF_2 for this interval. Their locations are listed in Table 1. Any data gaps (at most 3 years) were filled in using linear interpolation.

3. Methods

3.1. Ensemble Empirical Mode Decomposition

Empirical Mode Decomposition (EMD) is an algorithm to decompose a time series $x(t)$ into a finite number of Intrinsic Mode Functions (IMFs) and a residual [*Huang et al.*, 1998; *Huang and Wu*, 2008]. This can be written as

$$x(t) = \sum_{j=1}^{M} \psi_j(t) + R(t) \tag{2}$$

where $\psi_j(t)$ is the jth IMF, M is the total number of IMFs, and $R(t)$ is the residual. Each IMF can be written in polar coordinates:

$$\psi_j(t) = r_j(t) \sin\left(\theta_j(t)\right) \tag{3}$$

where $r_j(t)$ and $\theta_j(t)$ are the amplitude and instantaneous frequency, respectively, of the jth IMF. Note that both the amplitude and the frequency of each IMF are time dependent; this is different from a Fourier decomposition.

An IMF is defined by the following two properties: (1) each IMF has exactly one zero crossing between two consecutive local extrema and (2) the local mean of each IMF is zero. To estimate the IMFs from a given time series, the following algorithm is used: (1) Find all maxima and minima of the time series. (2) Fit a cubic spline through all maxima and minima; these splines define the upper e_{up} and lower e_{lo} envelopes of the time series. (3) Calculate the mean of the upper and lower envelope

$$m(t) = \left[e_{up}(t) + e_{lo}(t)\right]/2 \tag{4}$$

(4) Subtract $m(t)$ from the time series; the resulting curve $x(t) - m(t)$ is the first IMF. Then go back to 1 and repeat the procedure until $x(t) - m(t)$ no longer satisfies the criteria of an IMF. The remainder is the residual $R(t)$.

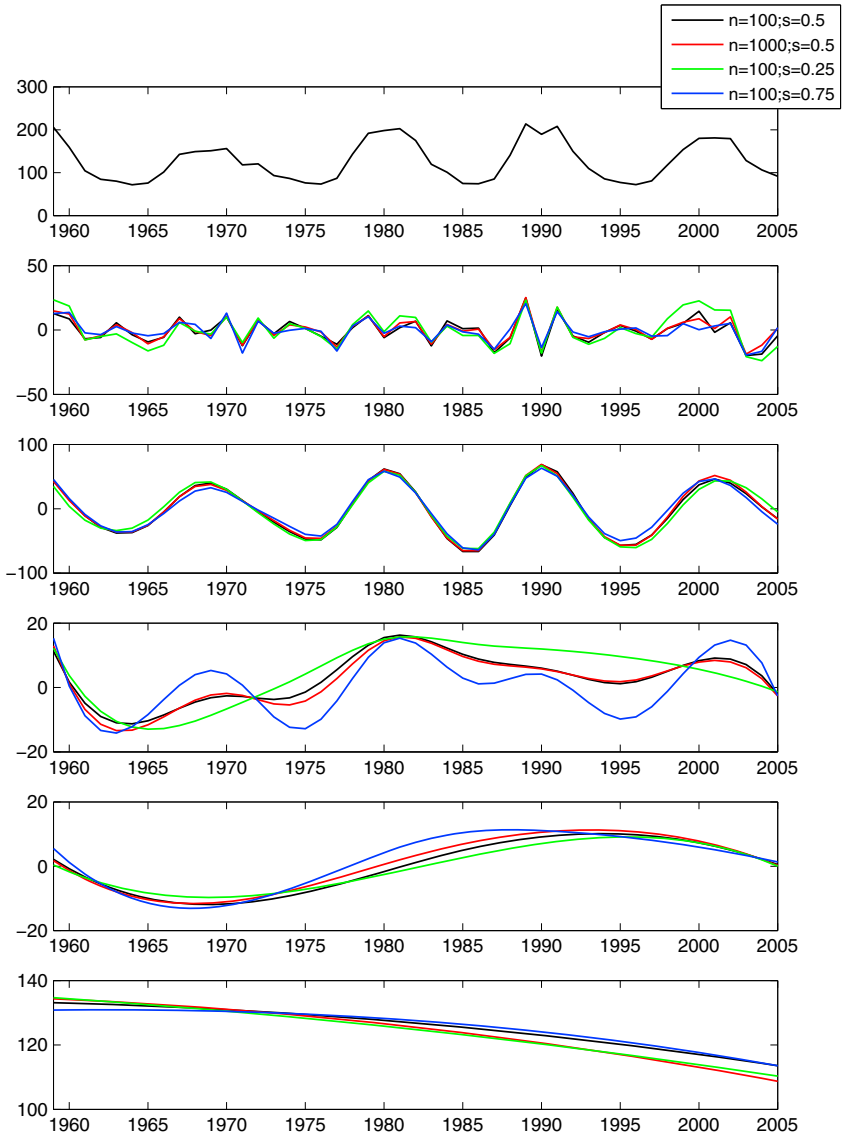

Figure 2. (first row) The original $F_{10.7}$ time series, (second to fifth rows) its IMFs, and (sixth row) the residual obtained with four different combinations of EEMD parameter settings; "*n*" is the number of ensembles and "*s*" the fraction of the standard deviation used as noise. Note that the EEMD analysis indicates a long-term decrease in solar activity.

In practice, the algorithm has to be refined by a so-called "sifting" process, which amounts to iterating steps 1–3 until a zero mean of the IMF has been realized to some stopping criterion [*Huang et al.,* 1998; *Rilling et al.,* 2003]. Once this has been achieved, the effective IMF has been determined. The residual that remains when all IMFs have been extracted this way can be interpreted as the instantaneous mean of the time series. The instantaneous mean can be a constant, a smooth monotonic function, or a smooth function with at most one extremum [*Huang and Wu*, 2008]. When the instantaneous mean is not constant, we refer to it as a trend.

A drawback of EMD analysis is that mode mixing can occur. This is defined as either a single IMF consisting of signals of widely disparate scales or a signal of similar scale residing in different IMF components. To suppress this problem, a variation on the original EMD technique, called Ensemble Empirical Mode Decomposition (EEMD), was introduced by *Wu and Huang* [2009]. In EEMD analysis, an ensemble is created by adding different white noise to the original time series before the sifting process. The original EMD algorithm is then applied to each ensemble member, and the ensemble means are treated as the final result. The rationale behind this is that only the true components of the time series will survive and persist in the final ensemble mean. Here we therefore used EEMD analysis.

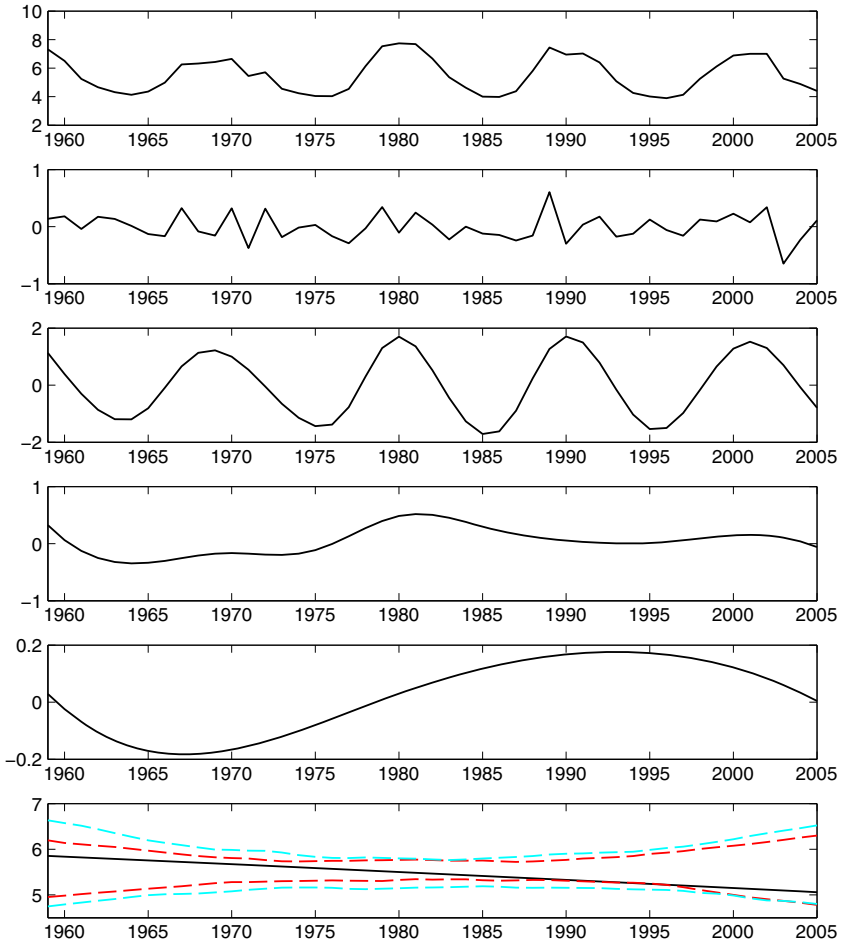

Figure 3. Example of the EEMD analysis applied to f_oF_2 data from Juliusruh/Rugen (same data as used in Figure 1a). (first row) The original f_oF_2 time series, (second to fifth rows) its IMFs, and (sixth row) the residual are shown. Figure 3 (sixth row) also indicates the 5–95% percentile ranges for both statistical null models: red, phase scrambling; cyan, AR process. In the example shown the residual (the trend) is just significant against the phase scrambling null model, but not against the AR null model.

The amplitude of the white noise to be added to the original time series needs to be finite, but not infinitesimal, so that the ensemble is forced to exhaust all possible solutions [*Huang and Wu*, 2008; *Wu and Huang*, 2009]. We experimented with different amplitudes of white noise, as well as different numbers of ensemble members, when applying EEMD to the $F_{10.7}$ time series. Some examples are shown in Figure 2. The second IMF appears to capture the 11 year solar cycle signal quite well, but for a high level of noise (0.75 times the standard deviation) some of this signal ends up partly in the third IMF. We consider it more desirable for the solar cycle signature to be associated with a single IMF and therefore eliminated this high noise level. When a low noise level of 0.25 times the standard deviation was used, we found that the result was relatively more sensitive to the number of ensemble members used (not shown) than at a noise level of 0.5 times the standard deviation. We therefore chose a noise level of 0.5 times the standard deviation. Also, at this noise level the residual in particular does depend somewhat on the number of ensemble members used, but the residual with 100 members does not look unreasonable compared to the other cases explored. In the interest of computational efficiency we therefore used 100 ensemble members for all further analyses. An example of the EEMD analysis with these settings applied to f_oF_2 data from Juliusruh/Rugen is shown in Figure 3. Also here, the second IMF clearly corresponds to the solar cycle signal.

3.2. Significance Testing

The significance of the trends obtained with the EEMD analysis was tested against two statistical null models. These null models were designed to share certain characteristics with the data, but they do not contain a

long-term trend by construction. They serve to define a distribution of trends that could reasonably be obtained from a time series with similar properties as the original data but containing no "true" trend. This allows us to gauge how likely it is that the trends obtained from the original data could have been produced by noise or stochastic processes, rather than indicating a significant, deterministic trend.

The first statistical null model makes use of phase scrambling [*Theiler et al.,* 1992; *Franzke*, 2012] to generate a time series with the same autocorrelation function and same probability density function as the original time series. This method first performs a Fourier transformation of the data. The autocorrelation function is uniquely defined by the amplitudes of the Fourier modes. To generate surrogate data, each complex Fourier amplitude is multiplied by $e^{i\varphi}$, where φ is independently chosen from a uniform distribution $U(0, 2\pi)$ for each frequency. Thus, the resulting time series is the sum of randomly phased Fourier components whose amplitudes satisfy the condition that the power spectrum of that time series is identical to the power spectrum of the original data time series (see *Theiler et al.* [1992] for more details).

The second statistical null model is a cyclic autoregressive (AR(1)) process [*Franzke*, 2013]. A cyclic AR(1) process is given by

$$x_{t+1} = \mu(T) + \alpha(T)x_t + \sigma(T)\varepsilon_t \tag{5}$$

where $\mu(T)$ is in our case the periodic mean solar cycle, $\alpha(T)$ is the periodic autoregressive parameter, $\sigma(T)$ the periodic standard deviation, ε_t is a normally distributed white noise variable, and T is the year. The parameters of the cyclic AR(1) model are estimated from the original time series by solving the periodic Yule-Walker equations for each T [*Franzke*, 2013].

For both statistical models we generated 100 realizations, which were subjected to the same trend analysis procedures as the original time series. If the trend obtained from the original data was outside the 5–95% percentile range of the synthetic trend distribution at any point, we considered it significant (see example in Figure 3). The same significance testing procedure was also applied to trends obtained with the linear regression approach to test the performance of the *F* test.

3.3. Data-Based Estimates of the Solar Contribution to Trends

There are a number of different ways to try and quantify the influence of long-term solar variability on trends in h_mF_2 and f_oF_2. Here we explore three different approaches, two of which are data based.

First, we employ a different correction for solar influences in the first step of the linear regression-based trend analysis. We noted already that the second IMF captures the solar cycle signal quite well, which is the dominant influence on h_mF_2 and f_oF_2. Therefore, we can use, instead of the original $F_{10.7}$ time series, only the second IMF to correct the h_mF_2 and f_oF_2 data to be analyzed. This way, the influence of the long-term decrease in solar activity should be retained. The difference between the trends obtained with this modified version of the linear regression-based trend analysis and the trends obtained with the standard linear regression analysis gives a first estimate of the contribution of long-term solar variation to trends in h_mF_2 and f_oF_2.

Second, we estimate the influence of the long-term trend in solar activity by taking the linear fit of the residual of the $F_{10.7}$ time series to obtain a trend in solar flux unit (sfu)/yr and multiplying this by a coefficient that describes the dependence of h_mF_2 or f_oF_2, respectively, on $F_{10.7}$. The linear fit is justified here because the $F_{10.7}$ residual is quite well described by a straight line. The coefficient we use to multiply with is the linear regression coefficient between the $F_{10.7}$ time series on the one hand and the h_mF_2 and f_oF_2 time series for each station on the other. This is not ideal, because h_mF_2 and f_oF_2 may respond differently to variations in $F_{10.7}$ on different time scales, as noted in the introduction. However, a better alternative is not readily available and it should still provide a useful additional estimate for comparison with our other estimates.

3.4. Numerical Model Simulations

Besides the data-based estimates of the contribution of long-term change in solar activity to trends in h_mF_2 and f_oF_2, we use two simulations with the thermosphere-ionosphere-electrodynamics general circulation model (TIE-GCM). The TIE-GCM is a time-dependent, three-dimensional model that solves the fully coupled, nonlinear, hydrodynamic, thermodynamic, and continuity equations of the thermospheric neutral gas self-consistently with the ion continuity equations. In the setup used here, the model grid consists of

Table 2. Trends in h_mF_2 (m/yr) Obtained With EEMD Analysis and Linear Regression Analysis and Their Significance[a]

	Trend (m/yr)	Significance		Linearity	Trend (m/yr)	Significance		
Station Name	EEMD	ph-scr	AR	R^2	Linear Regression	*F* Test	ph-scr	AR
Mawson	152.3			0.23	**490.2**	✓	✓	✓
Port Stanley	**−790.6**	✓	✓	**0.98**	**−471.8**	✓	✓	✓
Christchurch	**−177.0**	✓		**0.44**	321.9	✓		
Hobart	−347.2			0.86	27.9			
Canberra	−82.8			0.11	17.2			
Mundaring	**251.9**	✓	✓	**0.19**	235.4	✓		
Townsville	−161.5			0.99	−26.9			
Okinawa	80.4			0.31	146.2			
Hiratsuka	**−911.1**	✓	✓	**0.99**	**−481.7**	✓	✓	✓
Kokubunji	**−645.4**	✓	✓	**1.00**	**−304.4**	✓	✓	✓
Ashkabad	1.6			−0.02	265.0			
Boulder	**−666.1**	✓	✓	**0.94**	**−469.0**	✓	✓	✓
Rome	**−831.8**	✓	✓	**0.92**	**−651.6**	✓	✓	✓
Wakkanai	−237.5			0.75	**−310.6**	✓	✓	✓
Juliusruh/Rugen	**−523.3**	✓	✓	**0.95**	**−345.1**	✓	✓	✓
Moscow	−419.6			0.63	334.5	✓		
Tomsk	−455.9			0.98	−414.8	✓		
Leningrad	**−399.2**	✓		**0.87**	−108.7			
Sodankylä	**−410.7**	✓		**0.84**	**−397.6**	✓	✓	✓

[a]Trends that are significant against at least one of the statistical null models (ph-scr = phase scrambling; AR = cyclical AR process) are printed in bold. We also indicate that a trend is significant against the phase scrambling null model (columns 3 and 8), against the AR null model (columns 4 and 9), or according to the *F* test (column 7) using a tick mark (✓); nothing is printed in these columns if the trend is not significant. The linearity of the EEMD-derived trends is expressed by the adjusted R^2 value of a linear fit to those trends. The EEMD trend value at each station is the regression coefficient of that linear fit, used here as a measure of the magnitude of the trend.

36 latitude and 72 longitude points (5° × 5° resolution) and 29 pressure levels between ~96 km and ~500 km with a spacing of half a scale height. Information about the solar and geomagnetic activity levels is required as input; this can be specified through the $F_{10.7}$ index and the *Kp* index, respectively. The TIE-GCM is well established and has been widely used in the thermosphere-ionosphere community. We will therefore not give a full description here; more information can be found in *Roble et al.* [1988], *Richmond et al.* [1992], and *Qian et al.* [2014]. *Qian et al.* [2014] showed that the peak electron density in the F_2 layer, N_mF_2, simulated by the TIE-GCM is generally consistent with observations. Simulated electron density profiles at Millstone Hill also agree well with observations. This gives confidence that the TIE-GCM is a suitable model to use for our purposes.

The simulations used here were run from 1 March to 30 April, with prescribed solar activity levels. In one simulation $F_{10.7}$ was set constant at 130 sfu; in the other it was set constant at 110 sfu. These levels correspond roughly to the solar activity at the start and end points of the interval we study here (see Figure 2). We estimated the effect of such a change in solar activity level on h_mF_2 and f_oF_2 by averaging over all local times and taking the mean difference between the simulations over all days (61 in total). At each grid point, a *t* test was done to assess the statistical significance of the 61 day mean differences between the two simulations against day-to-day variability, represented by the standard deviation of the 61 values at that grid point. We used observed levels of geomagnetic activity (via the *Kp* index; here taken from 1 March to 30 April in 2008) to help achieve a realistic day-to-day variability. This is analogous to the procedure followed by *Cnossen* [2014]. The contribution of the long-term trend in $F_{10.7}$ to trends in h_mF_2 and f_oF_2 was estimated by dividing the 61 day mean differences by 47 (the number of years in our interval) at the grid points nearest to the stations selected for our analysis.

We note that by running the simulations only for equinox conditions rather than for a full year, the estimates obtained are not exactly comparable to the observed trends, which include data from the whole year. However, the simulation results still offer a useful guideline to the approximate effect of the long-term change in solar activity, independent of the ionosonde data on which our other estimates are based.

Table 3. Trends in f_oF_2 (kHz/yr) Obtained With EEMD Analysis and Linear Regression Analysis and Their Significance[a]

	Trend (kHz/yr)	Significance		Linearity	Trend (kHz/yr)	Significance		
Station Name	EEMD	ph-scr	AR	R^2	Linear Regression	*F* Test	ph-scr	AR
Syowa Base	**−45.5**	✓		**1.00**	**−26.4**	✓	✓	✓
Mawson	**−32.6**	✓	✓	**0.88**	**−19.6**	✓	✓	✓
Port Stanley	−17.6			1.00	**−8.2**	✓	✓	✓
Christchurch	**−11.8**	✓		**1.00**	−1.7			
Hobart	−7.0			1.00	−4.8	✓		
Canberra	−9.6			1.00	−5.0	✓		
Mundaring	−0.9			0.41	1.0			
Townsville	−7.0			0.48	4.4			
Okinawa	**−26.9**	✓		**0.96**	**−15.9**	✓	✓	✓
Yamagawa	−11.1			0.98	3.4			
Hiratsuka	−13.0			0.92	**−6.0**	✓		✓
Kokubunji	**−23.4**	✓	✓	**0.94**	**−9.3**	✓	✓	✓
Ashkabad	**44.2**	✓		**0.79**	39.6	✓		
Boulder	9.2			0.90	2.2			
Rome	**−13.5**	✓		**0.96**	**−4.4**	✓		✓
Wakkanai	**−17.5**	✓		**0.97**	−5.0	✓		
Juliusruh/Rugen	**−17.3**	✓		**1.00**	**−7.7**	✓	✓	
Moscow	−12.2			0.94	**−5.7**		✓	
Tomsk	**−25.9**	✓		**1.00**	**−20.8**	✓	✓	✓
Leningrad	**−21.6**	✓	✓	**0.99**	**−10.4**	✓	✓	✓
Sodankylä	**−22.3**	✓		**0.95**	**−14.1**	✓	✓	✓

[a]Trends that are significant against at least one of the statistical null models (ph-scr = phase scrambling; AR = cyclical AR process) are printed in bold. We also indicate that a trend is significant against the phase scrambling null model (columns3 and 8), against the AR null model (columns 4 and 9), or according to the *F* test (column 7) using a tick mark (✓); nothing is printed in these columns if the trend is not significant. The linearity of the EEMD-derived trends is expressed by the adjusted R^2 value of a linear fit to those trends. The EEMD trend value at each station is the regression coefficient of that linear fit, used here as a measure of the magnitude of the trend.

4. Results

4.1. Testing the Linear Regression Approach

One of the potential problems with the linear regression-based trend analysis approach is that it assumes that trends are linear over the time period considered. The EEMD method does not make this assumption. Instead, it allows us to quantify the linearity of the trends obtained with this method afterward by fitting straight lines to them. The adjusted R^2 value of the fit indicates the proportion of the trend that can be explained by that straight line. We use this as a measure of linearity.

Column 5 of Tables 2 and 3 shows the adjusted R^2 values for the straight-line fits to the EEMD-derived trends in h_mF_2 and f_oF_2, respectively. Of the trends in h_mF_2 that are significant against at least one of the statistical null models (10 in total), most are highly linear. The two exceptions are Christchurch ($R^2 = 0.44$) and Mundaring ($R^2 = 0.19$). However, examination of the h_mF_2 time series for Mundaring shows that there is an unusually low value for 1959, and because this happens to be the start point of our analysis, this has a rather large influence, making the overall trend significant and nonlinear. We tested whether the EEMD-based trend for Mundaring was still significantly positive when analyzing the period of 1960 to 2005 instead and found that this was not the case. Therefore, only the h_mF_2 trend for Christchurch appears to be reliably nonlinear. All of the trends in f_oF_2 that are significant against at least one of the statistical null models (12 in total) can be considered highly linear. The lowest R^2 value here is 0.79 for Ashkabad, and this result may in fact not be very reliable. The low R^2 for Ashkabad is mostly associated with unusually high f_oF_2 values between 1995 and 2005; nearly all of the trend is associated with this last decade, with hardly any change before 1995. We have some doubts over whether this trend is real. In general, the assumption of a linear trend therefore seems a reasonable one to make and should not introduce much error.

A second possible weakness of the linear regression approach is that the *F* test may not be entirely reliable, because its underlying assumptions are not strictly met by the data. To gauge how well the *F* test determines the statistical significance of trends obtained with the linear regression method, we compare the results of

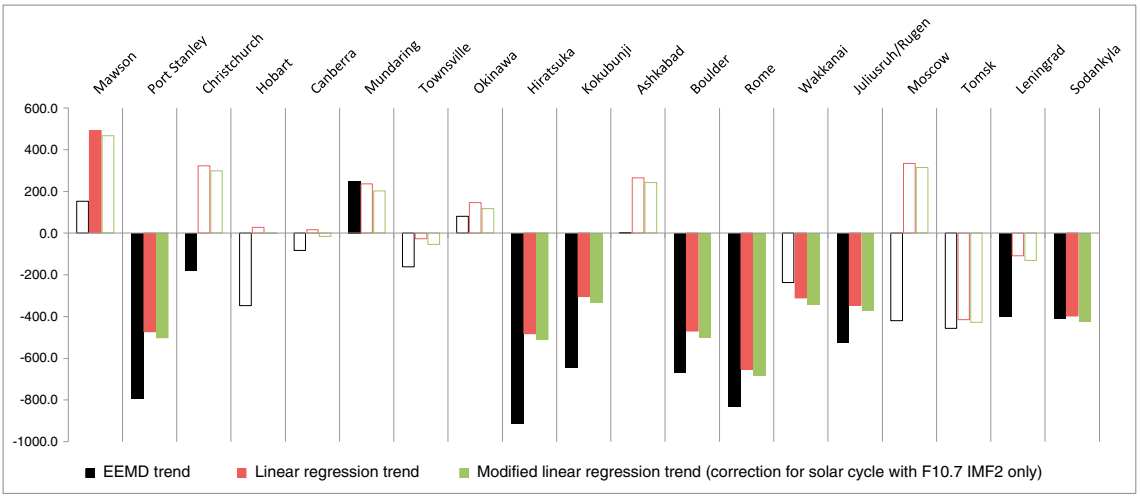

Figure 4. Trends in h_mF_2 (m/yr) obtained with the EEMD method (black), the standard linear regression method (red), and a modified linear regression method, where only IMF2 of the $F_{10.7}$ time series was used to correct for solar influences rather than the original $F_{10.7}$ time series (green; further discussed in section 4.3). Solid bars indicate trends that are significant against at least one of the statistical null models; open bars indicate nonsignificant trends.

the *F* test (column 7 of Tables 2 and 3) with significance against the phase scrambling and AR process null models (columns 8 and 9 of Tables 2 and 3). For h_mF_2, all trends that are significant against the phase scrambling and AR null models (nine in total) are also significant according to the *F* test. However, the *F* test reports in addition four trends as statistically significant which are not significant against either of the two statistical null models. For f_oF_2 all but one of the trends that are significant against at least one of the statistical null models (12 in total) are also significant according to the *F* test, Moscow being the exception. However, also in this case the *F* test reports four additional trends as statistically significant which are not significant against either of the two statistical null models.

4.2. Linear Regression Versus EEMD

So far we have not yet considered the magnitudes of the trends obtained. For trends obtained with the EEMD method there are different ways to define their magnitude. Given that most of the trends we obtained are highly linear, we have chosen here to use the slope of the straight-line fits mentioned earlier. These values, in m/yr for h_mF_2 and kHz/yr for f_oF_2, are shown in column 2 of Tables 2 and 3. Trends obtained with the linear regression approach (in the same units) are shown in column 6. Figures 4 and 5 compare trends obtained with these different methods visually.

For both h_mF_2 and f_oF_2 the EEMD-derived trends are noticeably more negative than those obtained with the standard linear regression method. This is the case for all of the trends that are significant against at least one of the statistical null models for both methods. Those trends are on average about 235 m/yr (h_mF_2) and 11 kHz/yr (f_oF_2) more negative for the EEMD analysis than they are for the linear regression analysis. These differences in trend magnitude between the two methods correspond to about 30–35% and almost 50% of the EEMD-derived trends in h_mF_2 and f_oF_2, respectively.

A possible explanation for the differences between the linear regression-based and EEMD-based trends may be found in the different treatment of solar influences. The linear regression method may result in less negative trends because the effect of the long-term decrease in solar activity (see Figure 2) has been corrected for before the final trend detection step, while any such influence is retained in the EEMD-derived trends. In the next section, we try to quantify the solar influence in several different ways.

4.3. Estimates of the Solar Contribution to Trends in h_mF_2 and f_oF_2

Our first estimate of the influence of the long-term trend in solar activity relies on a modification to the standard linear regression approach. As the second IMF captures the 11 year solar cycle signal quite well, we used, instead of the full $F_{10.7}$ time series, only its second IMF to correct the f_oF_2 and h_mF_2 time series. Any

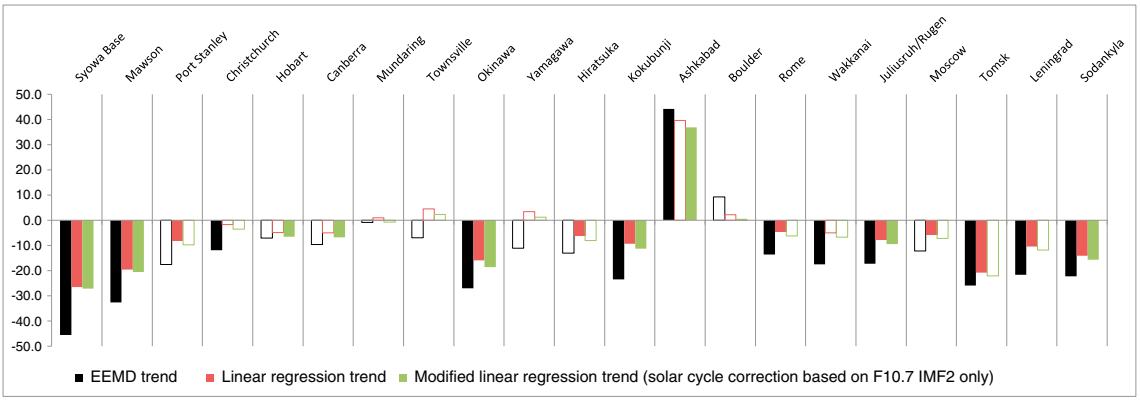

Figure 5. Trends in f_oF_2 (kHz/yr) obtained with the EEMD method (black), the standard linear regression method (red), and a modified linear regression method, where only IMF2 of the $F_{10.7}$ time series was used to correct for solar influences rather than the original $F_{10.7}$ time series (green; further discussed in section 4.3). Solid bars indicate trends that are significant against at least one of the statistical null models; open bars indicate nonsignificant trends.

influence of the long-term trend in solar activity should therefore now be retained. The trends obtained with this modified linear regression technique were already shown in Figures 4 and 5.

As expected, given the negative trend in $F_{10.7}$, the trends in both f_oF_2 and h_mF_2 are consistently more negative compared to those obtained with the standard linear regression approach. However, for h_mF_2 the difference between the two linear regression-based trends is only about 20–30 m/yr. Considering just significant trends, this tends to correspond to about 5–10% of the total trends in h_mF_2, so it is a relatively small difference. The differences in trends in f_oF_2 obtained with the two linear regression methods vary from <1 kHz/yr to >2.5 kHz/yr difference. This corresponds to anywhere between a few percent up to 20–30% of the total trends that are significant. The trends obtained with the modified version of the linear regression approach are still for the most part considerably more positive than the EEMD-derived trends.

A second way of estimating the influence of the long-term decrease in solar activity is through a multiplication of the straight-line fit of the $F_{10.7}$ residual, giving a trend in sfu/year, with the linear regression coefficient of the $F_{10.7}$ time series with the h_mF_2 and f_oF_2 time series for each station. Estimates obtained this way are shown in Figures 6 and 7. On average, the contribution of the long-term decrease in solar activity to the trends in h_mF_2 and f_oF_2 estimated this way is about -220 m/yr and about -12 kHz/yr, respectively. When only significant trends are considered, this corresponds to about 30–35% of the EEMD-derived trends for h_mF_2 and about 50%

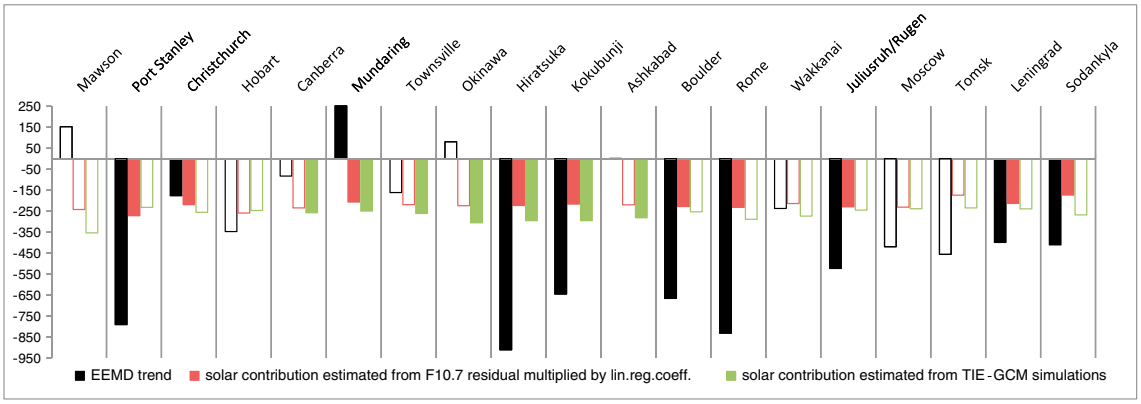

Figure 6. Trends in h_mF_2 (m/yr) obtained with the EEMD method (black) and estimates of the solar contribution to these trends based on multiplying the linear fit to the trend in $F_{10.7}$ with the linear regression coefficient between the $F_{10.7}$ and h_mF_2 time series (red) or on the basis of TIE-GCM simulations (green). For the EEMD trends (black) and the solar contribution estimated from the TIE-GCM simulations (green), solid bars indicate trends that are significant against at least one of the statistical null models or according to a t test, respectively, while open bars indicate nonsignificant trends. For the estimates of the solar contribution based on the trend in $F_{10.7}$ multiplied by the linear regression coefficient (red) we did not determine the statistical significance. Instead, bars are solid when the corresponding EEMD trend is significant against at least one of the statistical null models and open when it is not.

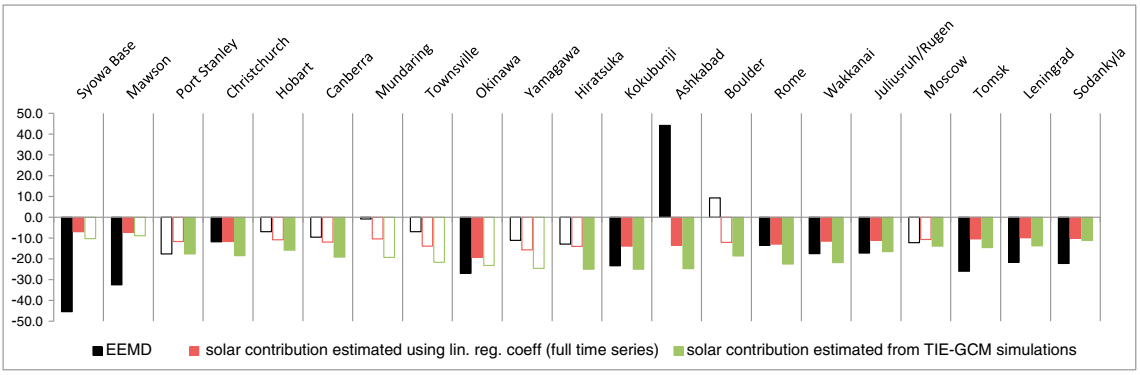

Figure 7. Trends in f_oF_2 (kHz/yr) obtained with the EEMD method (black) and estimates of the solar contribution to these trends based on multiplying the linear fit to the trend in $F_{10.7}$ with the linear regression coefficient between the $F_{10.7}$ and f_oF_2 time series (red) and on the basis of TIE-GCM simulations (green). For the EEMD trends (black) and the solar contribution estimated from the TIE-GCM simulations (green), solid bars indicate trends that are significant against at least one of the statistical null models or according to a *t* test, respectively, while open bars indicate nonsignificant trends. For the estimates of the solar contribution based on the trend in $F_{10.7}$ multiplied by the linear regression coefficients (red) we did not determine the statistical significance. Instead, bars are solid when the corresponding EEMD trend is significant against at least one of the statistical null models and open when it is not.

for f_oF_2. This estimate is considerably higher than the estimate obtained with the modified linear regression method. Interestingly, the new, higher estimate of the contribution of the long-term trend in solar activity corresponds very closely to the differences found between the trends obtained with the EEMD and linear regression analyses in section 4.2, both for h_mF_2 and f_oF_2.

A third way to estimate the influence of the change in solar activity is given on the basis of simulations with the TIE-GCM and is also shown in Figures 6 and 7. In general, this method estimates the solar contribution as somewhat higher still than the previous method: on average, the estimated contribution to trends in h_mF_2 and f_oF_2 is about −270 m/yr (~40% of the total EEMD-based trends) and about −19 kHz/yr (~80% of the total EEMD-based trends), respectively.

4.4. Comparisons Between Stations

Almost all of the trends in f_oF_2 that are significant are negative. The only exception is the trend in f_oF_2 for Ashkabad, which we consider to be not very reliable, as discussed in section 4.1. The largest significant trends in f_oF_2 are those for Syowa Base and Mawson, both high-latitude stations in the Southern Hemisphere. However, the number of significant trends is not sufficient to deduce reliably any systematic dependence on latitude. Trends at Okinawa and Kokubunji, both at relatively low latitudes, are of similar order of magnitude to those at higher latitude stations, such as Tomsk, Leningrad, and Sodankylä.

Trends in h_mF_2 are also nearly all negative. The only exceptions here are Mawson and Mundaring. We already discussed in section 4.1 that the trend for Mundaring is highly sensitive to inclusion/exclusion of the year 1959 and will therefore not discuss this further. The h_mF_2 time series for Mawson does not indicate any obvious problem, although there are considerable fluctuations from year to year. Also, the fact that only the linear regression analysis methods gives a significant trend means that there is some uncertainty as to whether this trend is real. If it is real, the difference with trends at the other stations is most likely due to its specific location. For instance, as a high-latitude station, Mawson may experience a different response to long-term changes in geomagnetic activity. Having said that, high-latitude stations in the Northern Hemisphere, such as Sodankylä and Leningrad, still show negative trends in h_mF_2, although these are somewhat weaker than significant negative trends found at midlatitude stations.

Only h_mF_2 for Christchurch appears to have a reliable nonlinear trend. The reason for this nonlinear trend compared to the highly linear trends found at most other stations is not clear. Two nearby stations, Canberra and Hobart, did not show a significant trend, and therefore, one may question whether the trend at Christchurch can be trusted. On the other hand, some drivers of long-term change (for instance, changes in the Earth's magnetic field) vary strongly with location and may show nonlinear changes in some, but not necessarily all, locations over the time period considered. The trend in h_mF_2 found at Christchurch could be indicative of such a (locally) nonlinear driver, but this would need further investigation to confirm.

5. Discussion

We applied EEMD analysis for the first time to ionosonde data to extract long-term trends in h_mF_2 and f_oF_2. We did this both to test some of the assumptions made by the more commonly used linear regression-based trend analysis and to reveal new information about the role of the Sun in long-term trends in h_mF_2 and f_oF_2.

Since EEMD analysis does not make any assumptions on the functional form of a trend, it was possible to quantify the linearity of the trends obtained afterward. This demonstrated that for most stations, trends in h_mF_2 and f_oF_2 are highly linear. In general, the assumption of linearity made by the linear regression-based trend analysis approach is therefore reasonable, at least for the interval studied here (1959–2005). However, there are exceptions for some stations, and this should be kept in mind.

We also tested the reliability of the *F* test, generally used to test for statistical significance as part of a linear regression-based trend analysis. Compared to the significance testing procedure adopted here, the *F* test tends to overestimate the statistical significance of trends; i.e., it reports some trends as significant that are not significant against either of the statistical null models we used. This occurred for about 25% of cases where the *F* test found a significant trend for f_oF_2 and about 30% of such cases for h_mF_2. This means that some of the trends reported in the literature as statistically significant based on the *F* test may not pass a harder test for statistical significance. Any such trends should be viewed with caution as they may not be reliably significant. In future work, it would be advisable to adopt a significance testing procedure as we have done here to avoid reporting questionable trends as significant [*Franzke*, 2012].

Comparing the trends obtained with linear regression and with EEMD analysis, we found that the latter were consistently more negative, by about 30–35% for h_mF_2 and almost 50% for f_oF_2. We explored whether this difference arises because the EEMD-based trends include the effect of a long-term decrease in solar activity, while this effect is removed from the trend obtained by linear regression. We estimated the effect of the long-term decrease in solar activity in three different ways, which gave considerably different results.

Interestingly, a multiplication of the EEMD-based trend in $F_{10.7}$ with the linear regression coefficient between the $F_{10.7}$ time series and the h_mF_2 and f_oF_2 time series for each station estimated the solar contribution at about 30–35% of the total EEMD-based trends in h_mF_2 and at about 50% of the total EEMD-based trends in f_oF_2. If this estimate is correct, the difference between the linear regression-based and EEMD-based trends could be entirely explained by the suggestion above, namely, that the linear regression-based analysis removes the influence of the long-term decrease in solar activity successfully, while this influence is retained by the EEMD analysis. On the other hand, it would also mean that the model simulations, which predicted a slightly larger solar contribution, overestimated the influence of the Sun, while our other data-based estimate of the solar contribution is too low. It is not entirely clear yet whether this is the correct interpretation.

All three estimates agree that the influence of the Sun is relatively more important for f_oF_2 than for h_mF_2. This fits in with h_mF_2 also being influenced by the increase in greenhouse gases, while this should not have a significant influence on f_oF_2 [*Rishbeth*, 1990; *Rishbeth and Roble*, 1992; *Cnossen*, 2014]. In relative terms, influences of other processes, such as long-term changes in solar activity, would therefore be expected to be more important for f_oF_2 than for h_mF_2.

6. Conclusions

Our main conclusions can be summarized as follows:

1. EEMD analysis shows that trends in h_mF_2 and f_oF_2 between 1959 and 2005 are in most cases highly linear. The assumption of a linear trend, often made by the linear regression-based trend analysis method, is therefore mostly a reasonable one.
2. The *F* test, generally used to test for statistical significance as part of a linear regression-based trend analysis, tends to overestimate statistical significance. Any published trends that were reported as significant based on this test should therefore be treated with caution. For future studies we recommend adopting a more rigorous significance testing procedure, such as we have done here.

3. Based on three different methods, we estimate that the trend in solar activity between 1959 and 2005 can explain between 5–10% and 35–40% of the total EEMD-based trends in h_mF_2 while this is estimated to be between 20–30% and up to as much as 80% for EEMD-based trends in f_oF_2. All three methods indicate that the influence of the Sun is relatively more important for long-term trends in f_oF_2 than for trends in h_mF_2.

Acknowledgments

This study is part of the British Antarctic Survey Polar Science for Planet Earth Programme. Ingrid Cnossen was sponsored by Natural Environment Research Council (NERC) fellowship NE/J018058/1. Christian Franzke was supported by the German Research Foundation (DFG) through the cluster of excellence Climate System Analysis and Prediction (CliSAP). The TIE-GCM simulations used in this study were performed on the Yellowstone high-performance computing facility (ark:/85065/d7wd3xhc) provided by NCAR's Computational and Information Systems Laboratory, sponsored by the National Science Foundation. Simulation results will be made freely available on request (contact the corresponding author if interested). We are grateful for the efforts of the ionosonde stations in collecting the data which made this study possible.

Michael Liemohn thanks Ana Elia, Alan Burns, and another reviewer for their assistance in evaluating the paper.

References

Bremer, J. (1992), Ionospheric trends in mid-latitudes as a possible indicator of the atmospheric greenhouse effect, *J. Atmos. Terr. Phys.*, *54*(11–12), 1505–1511.

Bremer, J., T. Damboldt, J. Mielich, and P. Suessmann (2012), Comparing long-term trends in the ionospheric F_2-region with two different methods, *J. Atmos. Sol. Terr. Phys.*, *77*, 174–185.

Cnossen, I. (2014), The importance of geomagnetic field changes versus rising CO_2 levels for long-term change in the upper atmosphere, *J. Space Weather Space Clim.*, *4*, A18, doi:10.1051/swsc/2014016.

Cnossen, I., and A. D. Richmond (2008), Modelling the effects of changes in the Earth's magnetic field from 1957 to 1997 on the ionospheric h_mF_2 and f_oF_2 parameters, *J. Atmos. Sol. Terr. Phys.*, *70*, 1512–1524.

Cnossen, I., and A. D. Richmond (2013), Changes in the Earth's magnetic field over the past century: Effects on the ionosphere-thermosphere system and solar quiet (Sq) magnetic variation, *J. Geophys. Res. Space Physics*, *118*, 849–858, doi:10.1029/2012JA018447.

Damboldt, T., and P. Suessmann (2012), Consolidated database of worldwide measured monthly medians of ionospheric characteristics f_oF_2 and M(3000)F_2, INAG Bulletin on the Web, INAG-73.

Elias, A. G., and N. Ortiz de Adler (2006), Earth magnetic field and geomagnetic activity effects on long-term trends in the F_2 layer at mid-high latitudes, *J. Atmos. Sol. Terr. Phys.*, *68*(17), 1871–1878.

Emmert, J. T., and J. M. Picone (2011), Statistical uncertainty of 1967–2005 thermospheric density trends derived from orbital drag, *J. Geophys. Res.*, *116*, A00H09, doi:10.1029/2010JA016382.

Franzke, C. (2010), Long-range dependence and climate noise characteristics of Antarctic temperature data, *J. Clim.*, *23*, 6074–6081.

Franzke, C. (2012), Nonlinear trends, long-range dependence, and climate noise properties of surface temperature, *J. Clim.*, *25*, 4172–4183.

Franzke, C. (2013), Significant reduction of cold temperature extremes in the Antarctic Peninsula at Faraday/Vernadsky Station, *Int. J. Clim.*, *33*, 1070–1078, doi:10.1002/joc.3490.

Huang, N. E., and Z. Wu (2008), A review on Hilbert-Huang transform: Method and its application to geophysical studies, *Rev. Geophys.*, *46*, RG2006, doi:10.1029/2007RG000228.

Huang, N. E., Z. Sheng, S. R. Long, M. C. Wu, H. H. Shih, Q. Zheng, N.-C. Yen, C. C. Tung, and H. H. Liu (1998), The empirical mode decomposition and the Hilbertspectrum for nonlinear and non-stationary time series analysis, *Proc. R. Soc. London A*, *454*(1971), 903–995.

Laštovička, J. (2005), On the role of solar and geomagnetic activity in long-term trends in the atmosphere-ionosphere system, *J. Atmos. Sol. Terr. Phys.*, *67*, 83–92.

Qian, L., A. G. Burns, B. A. Emery, B. Foster, G. Lu, A. Maute, A. D. Richmond, R. G. Roble, S. C. Solomon, and W. Wang (2014), The NCAR TIE-GCM: A community model of the coupled thermosphere/ionosphere system, in *Modeling the Ionosphere-Thermosphere System*, *Geophys. Monogr. Ser.*, vol. 201, edited by J. D. Huba, R. W. Schunk, and G. Khazanov, pp. 73–83, AGU, Washington, D. C., doi:10.1002/9781118704417.ch7.

Richmond, A. D., E. C. Ridley, and R. G. Roble (1992), A thermosphere/ionosphere general circulation model with coupled electrodynamics, *Geophys. Res. Lett.*, *19*, 601–604, doi:10.1029/92GL00401.

Rilling, G., P. Flandrin, and P. Goncalves (2003), On empirical mode decomposition and its algorithms, in *Proceedings of the 6th IEEE/EURASIP Workshop on Nonlinear Signal and Image Processing (NSIP'03)*, pp. 8–11, Grado, Italy.

Rishbeth, H. (1990), A greenhouse effect in the ionosphere?, *Planet. Space Sci.*, *38*(7), 945–948.

Rishbeth, H., and R. G. Roble (1992), Cooling of the upper atmosphere by enhanced greenhouse gases—Modelling of thermospheric and ionospheric effects, *Planet. Space Sci.*, *40*(7), 1011–1026.

Roble, R. G., and R. E. Dickinson (1989), How will changes in carbon dioxide and methane modify the mean structure of the mesosphere and thermosphere?, *Geophys. Res. Lett.*, *16*, 1441–1444, doi:10.1029/GL016i012p01441.

Roble, R. G., E. C. Ridley, A. D. Richmond, and R. E. Dickinson (1988), A coupled thermosphere/ionosphere general circulation model, *Geophys. Res. Lett.*, *15*, 1325–1328, doi:10.1029/GL015i012p01325.

Shimazaki, T. (1955), World wide daily variations in the height of the maximum electron density in the ionospheric F_2 layer, *J. Radio Res. Lab.*, *2*, 85–97.

Theiler, J., S. Eubank, A. Longtin, B. Galdrikian, and J. Doyne Farmer (1992), Testing for nonlinearity in time series: The method of surrogate data, *Physica D*, *58*, 77–94.

Ulich, T., and E. Turunen (1997), Evidence for long-term cooling of the upper atmosphere in ionosonde data, *Geophys. Res. Lett.*, *24*, 1103–1106, doi:10.1029/97GL50896.

Upadhyay, H. O., and K. K. Mahajan (1998), Atmospheric greenhouse effect and ionospheric trends, *Geophys. Res. Lett.*, *25*, 3375–3378, doi:10.1029/98GL02503.

Wu, Z., and N. E. Huang (2009), Ensemble empirical mode decomposition: A noise-assisted data analysis method, *Adv. Adapt. Data Anal.*, *1*(1), 1–41.